SLAC-PUB-348
September 1967

Y^* Production in 2.1 and 2.65 GeV/c K^-n Interactions*

by

G. B. Chadwick, Z. G. T. Guiragossián, and E. Pickup
Stanford Linear Accelerator Center, Stanford, California

and

A. Barbaro-Galtieri, M. J. Matison, and A. Rittenberg
Lawrence Radiation Laboratory, Berkeley, California

(Submitted to the Heidelberg International Conference
on Elementary Particles, September 20-27, 1967)

*Work supported by U. S. Atomic Energy Commission

X

We have studied the Σ^- and Λ^o/Σ^o producing channels of K^- deuterium interactions at 2.1 and 2.65 GeV/c incident momenta, in the LRL 72-inch deuterium bubble chamber. Among the 3- and 4-prong topologies containing a negatively charged decay, a total of 5822 events resulted in successful measurement, reconstruction and kinematical fits. In this sample, we discuss the reactions:

1. $K^-d \rightarrow \Sigma^- \pi^+ \pi^- [p]$
2. $K^-d \rightarrow \Sigma^- \pi^+ \pi^o \pi^- [p]$

Furthermore, the 1- and 2-prong with a V_o topologies gave a total of 12,623 successfully processed events. Here, the reactions of interest are:

3. $K^-d \rightarrow \Lambda^o \pi^- \pi^o [p]$
4. $K^-d \rightarrow \Lambda^o \pi^-$ MM $[p]$

To obtain reasonable statistics while maintaining the validity of the impulse approximation, the odd-prong events with invisible spectator protons were included in the sample, and hypothesized to have zero measured momentum with an error of ~40 MeV/c – the range of 2 mm in deuterium; and fitted as such.

From a study of the resulting fitted momenta of these spectators and a comparison of the general features of the channels with events having visible recoils less than 280 MeV/c, we believe that the data presents a true picture in reactions 1-4. Also, we have examined the strange-particle life-time distributions in each of the reactions and have found no significant biases which alter our conclusions.

Further, the ambiguities among several hypothesized fits in each of the topologies were resolved and the general consistency of the fits were checked on the scanning table for all events in this sample.

We find that the mass resolution broadening in the 1C and 0C reactions is primarily due to the invisible spectators and in some cases to the dual nearby Σ^- solutions. An estimate of this broadening for such reactions can be obtained by

comparing the experimental widths of the η^o and ω^o in this experiment, given in Table II, with the widths observed in hydrogen experiments.

Figure 1 shows the Dalitz plot for reaction (1) at 2.1 GeV/c, along with the mass projections in $\Sigma^- \pi^+$, $\Sigma^- \pi^-$, and $\pi^+ \pi^-$. Figure 2 shows the Dalitz plot for reaction (1) at 2.65 GeV/c along with similar projections. The presence of Y^* and boson resonances and the effects of their reflections have been studied with the aid of the FORTRAN program MURTLEBERT.[1] This program fits the data in all channels at once, using the Maximum Likelihood method, according to a given model. We assume that the reactions at our energies are adequately modeled by phase space and Breit-Wigner resonances. The amounts, masses and widths of several resonances can be varied and their appropriate reflections taken into consideration.

Table I summarizes the various channel cross sections, giving also the mass, experimental width and amount of resonant states at both energies. The only significant difference between our values and those well established in the literature is in the width of the $Y^*_{0,1}(1670)$, which is ~40 MeV wider. K^-p and K^-d total cross section counter measurements[4] indicate the presence of a $Y^*_0(1690)$, Γ = 40 MeV. Therefore the broadening of our 1670 peak could be due to the presence of both resonances in this region.

Figure 3 shows the Chew-Low scatter plots for the Y^*'s at 2.1 and 2.65 GeV/c. Figure 3(b) suggests that in the 2.65 GeV/c data at the mass region of 1670 there could be two clusters, a lower mass cluster at small momentum transfers $t[n, (\Sigma^- \pi^+)]$ and a higher mass cluster at large momentum transfers, corresponding to the $Y^*_1(1660)$ and $Y^*_0(1690)$, respectively. We note from these plots that only the $Y^*_0(1405)$ can be explained by boson exchanges alone.

We now consider Y^* production in reaction (2). Figure 4(a,b) shows $Y_1^*(1385)$ production in the $\Sigma^-\pi^0$ spectrum; some $Y_1^*(1660)$ could be present in the 2.1 GeV/c data, although the fit does not necessarily require the presence of this.

Figure 5 (a,b) shows the $\Sigma^-\pi^+$ mass spectrum, where $Y_0^*(1405)$ and $Y_0^*(1520)$ are observed at both momenta. In addition, Fig. 5(b) has $Y_{0,1}^*(1660)$ with an experimental width of $\Gamma = 45$ MeV.

Table II summarizes the several channels of reaction (2) listing the fitted amounts and resonance parameters.

One of the motivations for the study of reaction (1) has been the investigation of a possible $I = 2$ hyperon state[2] which in our case would unambiguously decay into $\Sigma^-\pi^-$. The presence of such a state is permitted by SU(3) considerations in a 27 multiplet representation. However, the simple quark model of $q_1q_2q_3$ representation for baryons, strictly forbids the presence of any state with isospin > 3/2. A recent investigation[3] of reaction (1) in (K^-,n) CM energy range of 1670-1860 MeV set an upper limit of 20 μb for a $Y_2^*(1415)$ production, although this energy range is dominated by s-channel Y_1^* resonance formation.

Figures 1(b) and 2(b) show the $(\Sigma^-\pi^-)$ distribution at 2.1 and 2.65 GeV/c, along with the predicted reflections. While there are no significant peaks seen in these distributions, consideration of fluctuations would set an upper limit of 13 ± 5 μb on any possible $\Sigma^-\pi^-$ effect. However, $SU(6)_W$ considerations[6] may make it more significant to look at three particle decay modes. As such we don't see anything immediately significant in our $\Sigma^-\pi^-\pi^0$ spectrum.

Finally, we discuss reactions (3) and (4) in a very specific sense. Reaction (4) may contain the final states of

(5a) $K^-d \rightarrow \Sigma^0\pi^0\pi^-$ [p]

(5b) $K^-d \rightarrow \Lambda^0\pi^-\pi^0\pi^0$ [p]

along with

$$(5c)\quad K^- d \longrightarrow \Lambda^0 \pi^- n(\pi^0)\,[p]\,,\ n > 2.$$

Through judicious usage of kinematical relations[7] and the known masses in the reaction and decay components of (5a), we may evaluate $\cos\theta_{\Sigma^0\gamma}$. This is the angle between the line of flight of Σ^0 from the $(\Sigma^0\pi^0)$ rest frame and γ in the decay of $\Sigma^0 \longrightarrow \Lambda^0\gamma$, evaluated in the Σ^0 rest frame. The angular distribution in $\cos\theta_{\Sigma^0\gamma}$, for reactions (5b) or (5c), yields some continuous reflection of the missing mass spectrum at $\cos\theta_{\Sigma^0\gamma} > 1.0$. Further, an essential δ function should be obtained at -1.0 if the missing mass is equal to a single π^0.

We summarize the kinematical relations:

$$\cos\theta_{\Sigma^0\gamma} = \frac{M^2(MM) - m^2_{\pi^0} - 2\epsilon\omega_{\pi^0}}{2\left|\vec{K}_{\pi^0}\right|\epsilon}$$

where ω_{π^0}, $\left|\vec{K}_{\pi^0}\right|$ = energy, momentum of the π^0 in reaction (5a), evaluated in the Σ^0 rest frame, and ϵ = γ energy in the same frame, i.e., the canonical 74.5 MeV in Σ^0 decays.

$$\omega_{\pi^0} = \frac{E_{\pi^0}\, M(\Lambda^0 MM) - m^2_{\pi^0}}{M_{\Sigma^0}}$$

where E_{π^0}, $\left|\vec{q}_{\pi^0}\right|$ = energy, momentum of the π^0 in reaction (5a), evaluated in the $(\Sigma^0\pi^0)$ rest frame; that is

$$E^2_{\pi^0} = q^2_{\pi^0} + m^2_{\pi^0}$$

$$q^2_{\pi^0} = \frac{1}{4}\left[M^2(\Lambda^0 MM) - 2\left(M^2_{\Sigma^0} + m^2_{\pi^0}\right) + \frac{\left(M^2_{\Sigma^0} - m^2_{\pi^0}\right)^2}{M^2(\Lambda^0 MM)}\right]$$

Thus the Σ^0 decay angle can be evaluated as a function of measurable and known quantities. Figure 6(d) shows this angular distribution for our entire sample of reaction (3) and (4). Here, we have removed all possible $Y_1^*(1385)$ events in the $(\Lambda^0\pi^-)$ mass combination, and the sample contains both invisible spectator protons with momenta set to zero MeV/c, and visible recoils with momenta less than 280 MeV/c. Aside from the peak broadening of the single π^0 events, due mostly to the zero momentum value of the invisible recoils, a clear plateau is observed in the physical region of $\cos\theta_{\Sigma^0\gamma}$ corresponding to the presence of reaction (5a).

Figure 6(b) is the same angular distribution with only the sample of visible recoils. The peak corresponding to single π^0 events is considerably sharpened.

On the basis of this, the angular region of $-0.70 < \cos\theta_{\Sigma^0\gamma} < 1.0$ is selected to yield an enriched sample of reaction (5a). We note that the major contaminant to reaction (5a) is primarily the reaction (5b). However, states that decay into $\Sigma^0\pi^0$ and $\Lambda\pi^0\pi^0$ must necessarily be isoscalars.

Figure 6(c) shows the $\Sigma^0\pi^0$ mass spectrum for these events. A clear signal at the 1520 and the region of 1800 is observed. We note that, based upon the experimental width of the 1520, our mass resolution is ~ 40 MeV.

Further study of this challenging method may reveal other isoscalar hyperons.

REFERENCES

1. J. Friedman, Lawrence Radiation Laboratory Document APG Note P-156 (1966).
2. Y. L. Pan and R. P. Ely, Phys. Rev. Letters 13, 277 (1964).
3. R. B. Bell, R. P. Ely, and Y. L. Pan, Phys. Rev. Letters 18, 921 (1967).
4. J. D. Davies *et al.*, Phys. Rev. Letters, 18, 62 (1967).
5. G. B. Chadwick, Z. G. T. Guiragossián, E. Pickup, A. Barbaro-Galtieri, M. J. Matison, and A. Rittenberg, SLAC-PUB-347, Stanford Linear Accelerator Center, Stanford University, Stanford, California (1967).
6. D. Horn, H. J. Lipkin, and S. Meshkov, Phys. Rev. Letters 17, 1200 (1966).
7. Z. G. T. Guiragossián, SLAC-TN-67-27, Stanford Linear Accelerator Center, Stanford University, Stanford, California (September 1967).

TABLE I

Channel cross sections and resonance parameters in $K^-d \rightarrow \Sigma^- \pi^+ \pi^0$ [p]

	Channel Parameters from MURTLEBERT Fit			σ μb
	M, MeV	Γ, MeV	Amount from fit, %	
2.1 GeV/c, $K^-n \rightarrow \Sigma^- \pi^+ \pi^-$				403
$K^-n \rightarrow \Sigma^- \rho^0$	760	120	34.4 ± 3.3	137 ± 25
$\rightarrow Y_0^* \pi^-$	1410	27	7.2 ± 1.2	28 ± 5
$\rightarrow Y_0^* \pi^-$	1520	15	18.5 ± 1.6	74 ± 10
$\rightarrow Y_{0,1}^{*0} \pi^-$	1670	90	17.0 ± 2.4	68 ± 15
$\rightarrow Y_0^* \pi^-$	1820	80	4.5 ± 2.0	18 ± 8
2.65 GeV/c, $K^-n \rightarrow \Sigma^- \pi^+ \pi^-$				264
$K^-n \rightarrow \Sigma^- \rho^0$	760	120	22.4 ± 3.2	59 ± 15
$\rightarrow Y_0^* \pi^-$	1410	44	11.2 ± 1.7	29 ± 5
$\rightarrow Y_0^* \pi^-$	1518	24	17.6 ± 2.0	46 ± 9
$\rightarrow Y_{0,1}^{*0} \pi^-$	1660	60	9.8 ± 2.0	26 ± 5
$\rightarrow Y_0^* \pi^-$	1820	80	11.7 ± 2.5	31 ± 8

TABLE II

Channel cross sections and resonance parameters in $K^-d \to \Sigma^-\pi^+\pi^0\pi^-[p]$

	Channel Parameters from MURTLEBERT Fit			σ μb
	M, MeV	Γ, MeV	Amount from fit, %	
2.1 GeV/c, $K^-n \to \Sigma^-\pi^+\pi^0\pi^-$				312
$K^-n \to \Sigma^-\eta^0$	548	50	4.4 ± 1.0	14 ± 3
$\to \Sigma^-\omega^0$	783	60	37.7 ± 3.3	118 ± 40
$\to \Sigma^- H^0$	996	80	12.0 ± 3.7	37 ± 11
$\to \Sigma^-\pi^0\rho^0$	760	100	4.3 ± 2.0	14 ± 6
$\to Y_1^*\pi^+\pi^-$, $\hookrightarrow \Sigma^-\pi^0$	1390	50	14.4 ± 3.0	45 ± 9
$\to Y_1^*\pi^-\pi^0$	1385	35	~ 3	~ 9
$\to Y_0^*\pi^-\pi^0$	1408	25	5.5 ± 2.0	17 ± 6
$\to Y_0^*\pi^-\pi^0$	1520	25	4.7 ± 2.0	15 ± 6
$\to Y_1^*\pi^-\pi^0$, $\hookrightarrow \Sigma^-\pi^+$	1660	45	-	-
2.65 GeV/c, $K^-n \to \Sigma^-\pi^+\pi^0\pi^-$				270
$K^-n \to \Sigma^-\eta^0$	548	50	5.0 ± 0.6	13.5 ± 2
$\to \Sigma^-\omega^0$	783	45	24.0 ± 1.0	65 ± 8
$\to \Sigma^- H^0$	990		difficult to estimate	
$\to \Sigma^-\pi^0\rho^0$	760	100	0	
$\to Y_1^{*-}\pi^+\pi^-$, $\hookrightarrow \Sigma^-\pi^0$	1385	35	13 ± 1.0	35 ± 5
$\to Y_0^*\pi^-\pi^0$	1405	30	3.5 ± 0.8	9 ± 3
$\to Y_0^*\pi^-\pi^0$	1522	30	5 ± 1.0	13.5 ± 3
$\to Y_1^*\pi^-\pi^0$	1660	45	5.8 ± 1.0	16 ± 3

$K^- d \rightarrow \Sigma^- \pi^+ \pi^-$ (p_s) 2.1 GeV/c (845 EVENTS)

(MASS HISTOGRAMS WITH "MURTLEBERT" FITS)

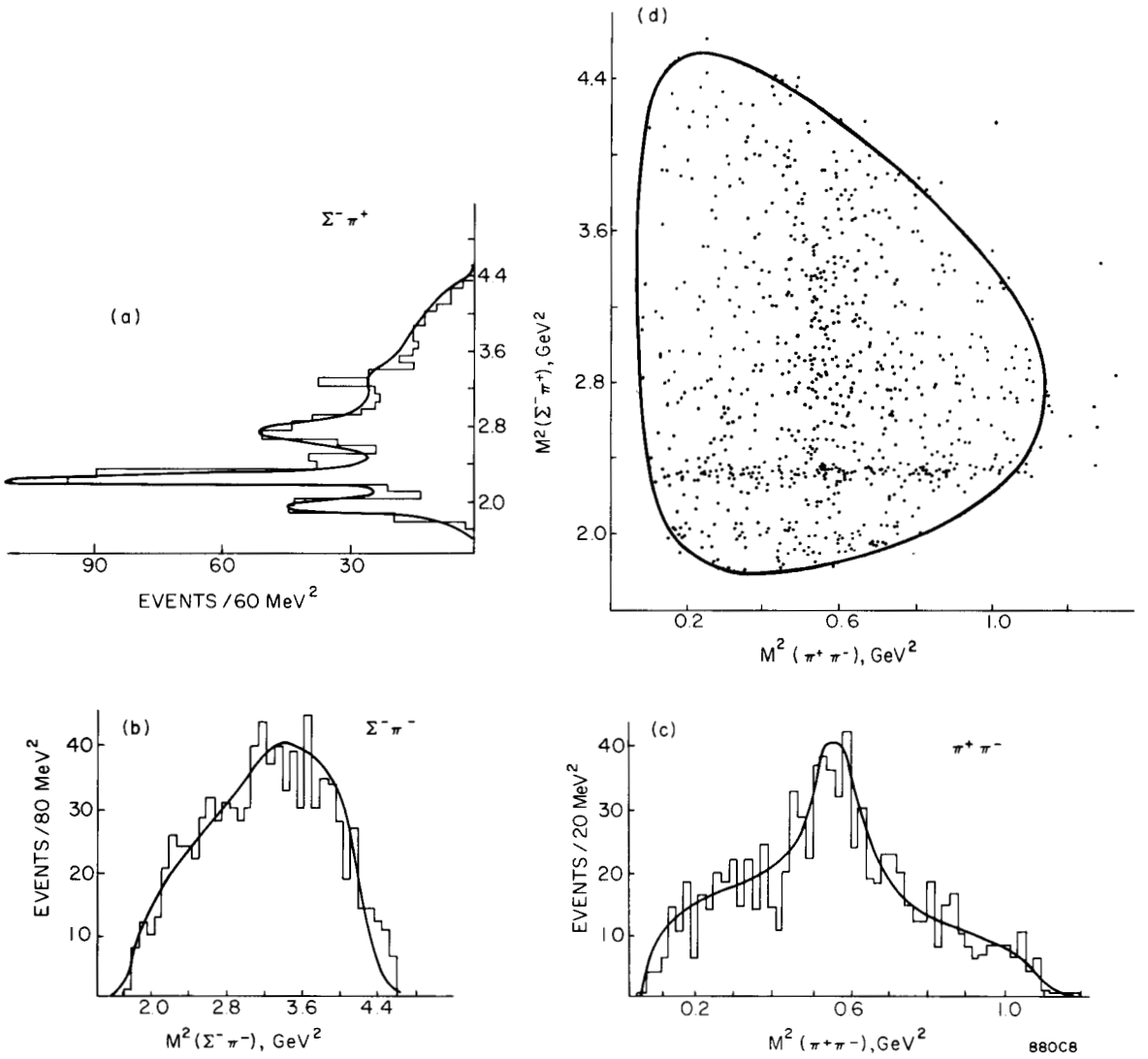

FIG. 1

K d—$\Sigma^- \pi^+ \pi^-$ (p_s) 2.65 GeV/c (596 EVENTS)
(MASS HISTOGRAMS WITH "MURTLEBERT" FITS)

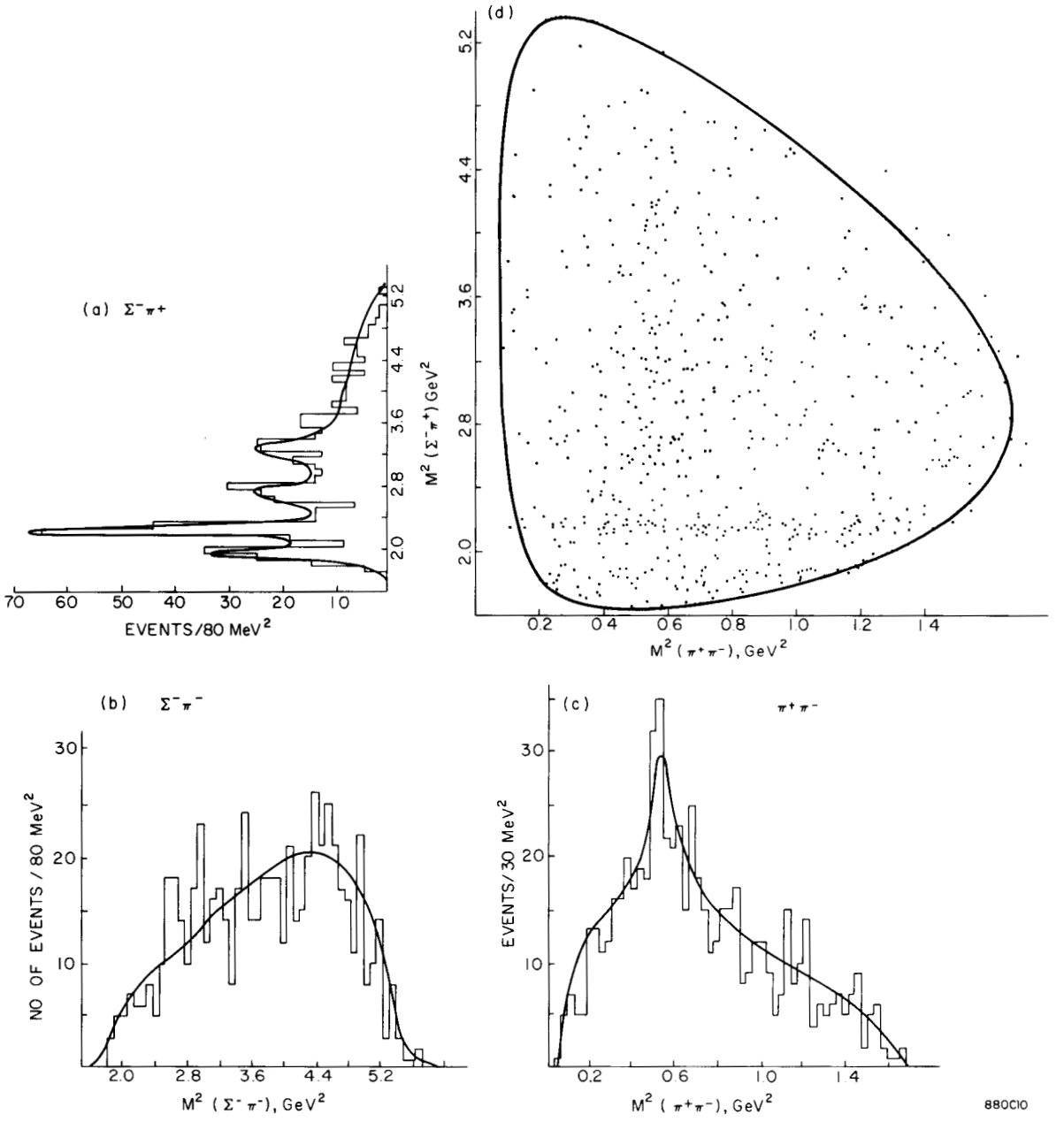

FIG. 2

$K^- n \to \Sigma^- \pi^+ \pi^-$, $t(n,[\Sigma^- \pi^+])$ vs $M^2(\Sigma^- \pi^+)$

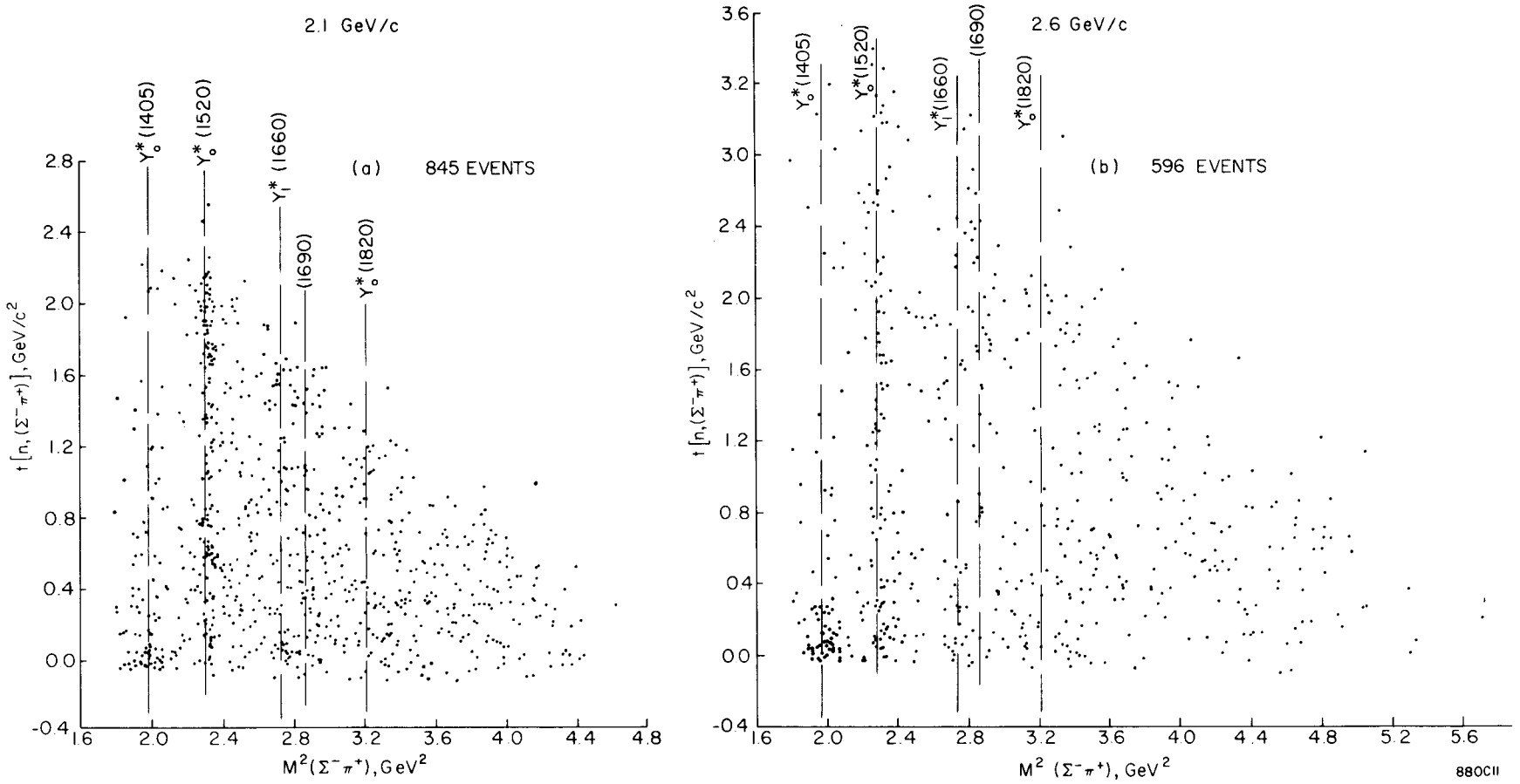

FIG. 3

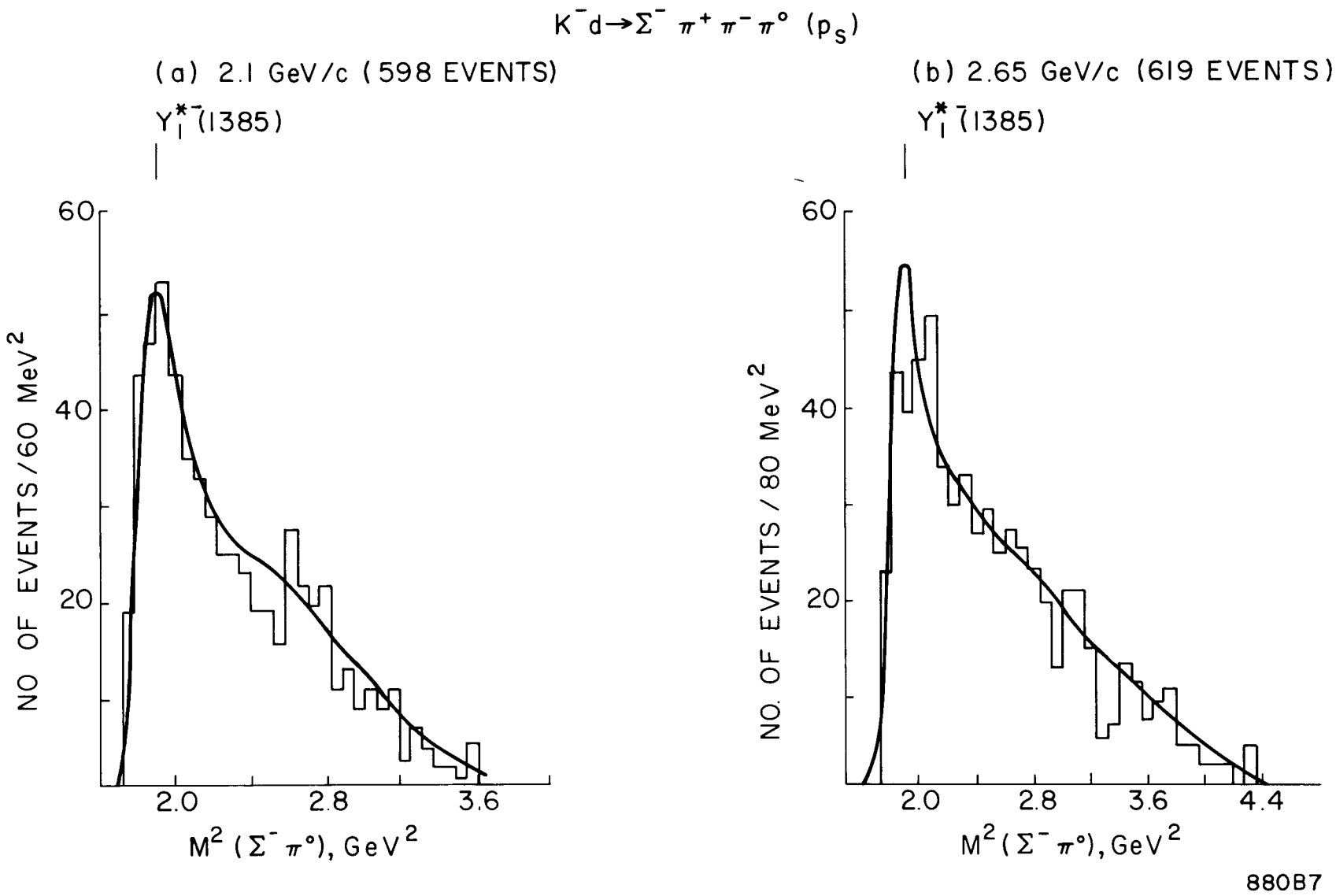
$K^- d \rightarrow \Sigma^- \pi^+ \pi^- \pi^0$ (p_s)
(a) 2.1 GeV/c (598 EVENTS)
$Y_1^{*-}(1385)$
NO OF EVENTS/60 MeV^2
60
40
20
2.0
2.8
3.6
$M^2(\Sigma^- \pi^0)$, GeV^2
(b) 2.65 GeV/c (619 EVENTS)
$Y_1^{*-}(1385)$
NO. OF EVENTS / 80 MeV^2
60
40
20
2.0
2.8
3.6
4.4
$M^2(\Sigma^- \pi^0)$, GeV^2
880B7

FIG. 4

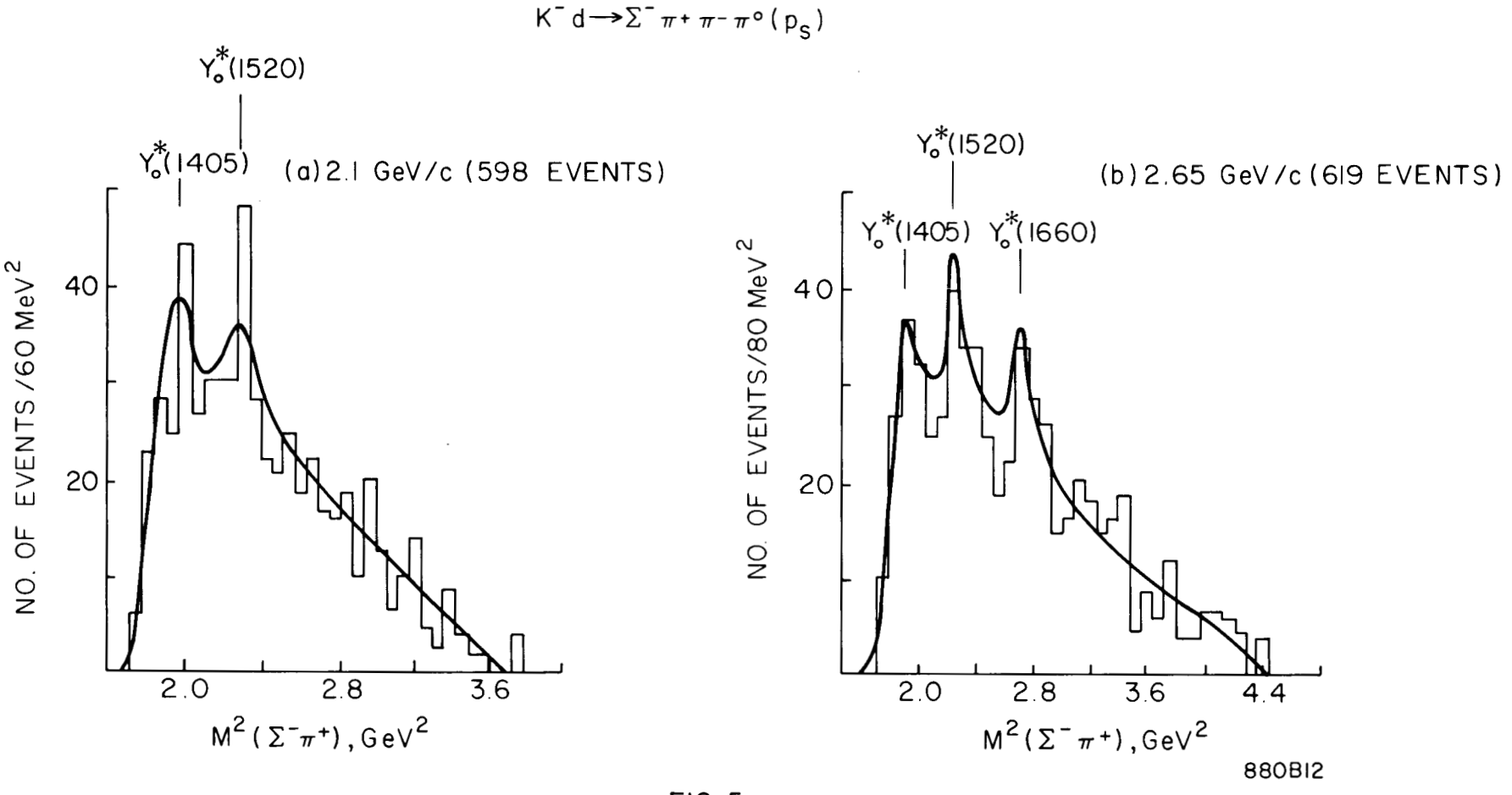
K⁻ d → Σ⁻ π⁺ π⁻ π⁰ (p_s)
Y₀*(1520)
Y₀*(1405)
(a) 2.1 GeV/c (598 EVENTS)
NO. OF EVENTS/60 MeV²
40
20
2.0
2.8
3.6
M²(Σ⁻π⁺), GeV²
Y₀*(1520)
(b) 2.65 GeV/c (619 EVENTS)
Y₀*(1405)
Y₀*(1660)
NO. OF EVENTS/80 MeV²
40
20
2.0
2.8
3.6
4.4
M²(Σ⁻π⁺), GeV²
880B12

FIG. 5

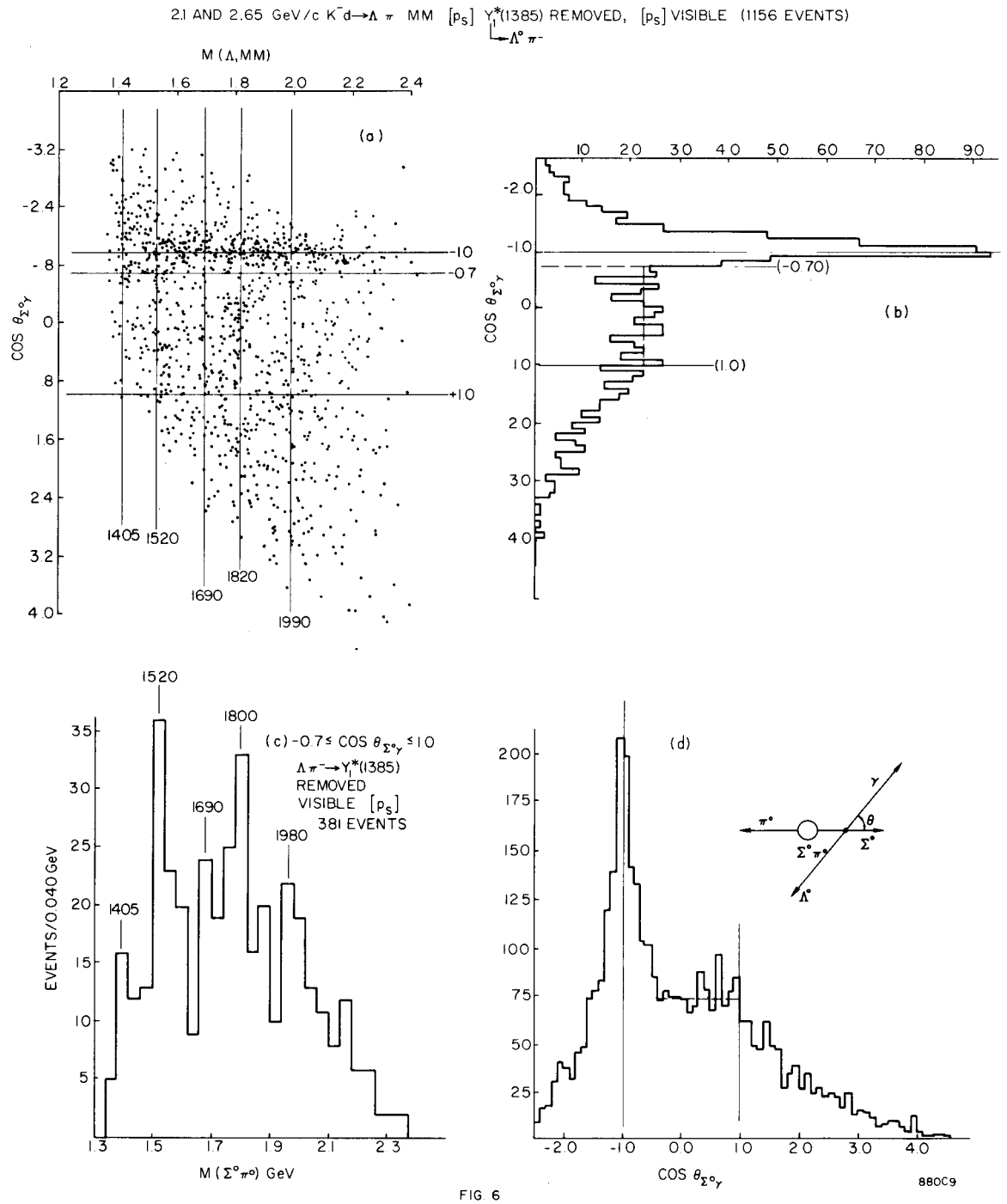
2.1 AND 2.65 GeV/c K⁻d→Λ π MM [ps] Y1*(1385) REMOVED, [ps] VISIBLE (1156 EVENTS)
Λ° π⁻
M (Λ,MM)
(a)
COS θΣ°γ
-1.0
-0.7
+1.0
1405
1520
1690
1820
1990
(b)
(-0.70)
(1.0)
(c) -0.7≤ COS θΣ°γ ≤1.0
Λπ⁻→Y1*(1385)
REMOVED
VISIBLE [ps]
381 EVENTS
1520
1800
1690
1980
1405
EVENTS/0.040 GeV
M (Σ°π°) GeV
(d)
γ
π°
θ
Σ°π°
Σ°
Λ°
COS θΣ°γ
880C9

FIG. 6